Chapter 5
Towards a Quantitative Understanding

Abstract Taking a binuclear copper complex as model system, the isotropic magnetic coupling is decomposed into different contributions. Perturbative expressions of the main contributions are derived and illustrated with numerical examples. An effective Hamiltonian is constructed that incorporates all important electron correlation effects and establishes a connection between the complex N-electron wave functions and the simpler qualitative methods discussed in the previous chapter. Subsequently an outline is given of the analysis of the coupling with a single determinant approach and the biquadratic and four-center interactions are decomposed. The chapter closes with the recently proposed method to extract DFT estimates for these complex interactions.

5.1 Decomposition of the Magnetic Coupling

The production of accurate electronic structure parameters is of course an important result for computational chemistry. However, it should not be the final goal and one has to go one step further on the road towards understanding. The qualitative valence methods described in the first sections of the previous chapter of this book are mainly focused on this understanding of the coupling, but here we discuss three approaches to analyse the results of the computational schemes that aim at a quantitative agreement with experiment. In this way quantitative accuracy can be combined with qualitative understanding.

The binuclear complex $[L_2Cu_2(\mu\text{-}1,3\text{-}N_3)_2]^{2+}$ (L = N,N',N''-trimethyl-1,4,7-triaza-cyclononane) shows a large antiferromagnetic coupling with $J = -800\,\text{cm}$, nicely reproduced with a DDCI calculation using a CAS(2,2)SCF reference wave function on the model complex $[(NH_3)_6Cu_2(\mu\text{-}1,3\text{-}N_3)_2]^{2+}$ [1]. In this section, we will closely follow the work of Calzado and co-workers, decompose this 800 cm^{-1} into small pieces and ascribe each individual contribution to well defined physical mechanisms [2, 3].

C. Graaf and R. Broer, *Magnetic Interactions in Molecules and Solids*,
Theoretical Chemistry and Computational Modelling,
DOI 10.1007/978-3-319-22951-5_5

5.1.1 Valence Mechanisms

First we focus on the mechanisms that arise from interactions among the configurations in the active space, restricting ourselves to the role played by the two Cu^{2+} ions. For this centro-symmetric system, the active orbitals $g = (a + b)/\sqrt{2}$ and $u = (a - b)/\sqrt{2}$ shown in Fig. 5.1 define four different determinants

$$\text{CAS} = \{|g\overline{g}|, |u\overline{u}|, |g\overline{u}|, |u\overline{g}|\} \tag{5.1}$$

The diagonalization of the corresponding 4×4 matrix produces four eigenstates, three singlets and one triplet

$$\begin{aligned} S_g &= \lambda|g\overline{g}| - \mu|u\overline{u}| \\ S'_g &= \mu|g\overline{g}| + \lambda|u\overline{u}| \\ T_u &= \big(|g\overline{u}| - |u\overline{g}|\big)/\sqrt{2} \\ S_u &= \big(|g\overline{u}| + |u\overline{g}|\big)/\sqrt{2} \end{aligned} \tag{5.2}$$

5.1 Demonstrate by substitution that S_g is dominated by the neutral determinants when $\lambda \approx \mu$. What situation is described for $\lambda \gg \mu$?

The energy difference of S_g and T_u defines J but the analysis is much easier in a representation with localized orbitals. Therefore, we rewrite the CAS in terms of the orthogonal localized Cu orbitals a and b, shown in Fig. 5.2. By defining the following electronic structure parameters

$$\begin{aligned} E_{ref} &= \langle a\overline{b}|\hat{H}|a\overline{b}\rangle = 0 \\ K_{ab} &= \langle a\overline{b}|\hat{H}|b\overline{a}\rangle \\ t_{ab} &= \langle a\overline{b}|\hat{H}|a\overline{a}\rangle \\ U &= \langle a\overline{a}|\hat{H}|a\overline{a}\rangle - \langle a\overline{b}|\hat{H}|a\overline{b}\rangle \end{aligned} \tag{5.3}$$

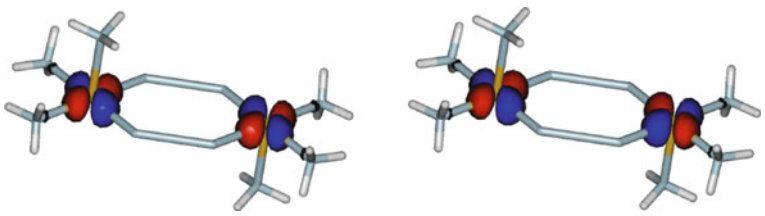

Fig. 5.1 Delocalized magnetic orbitals of *gerade* (*left*) and *ungerade* (*right*) symmetry

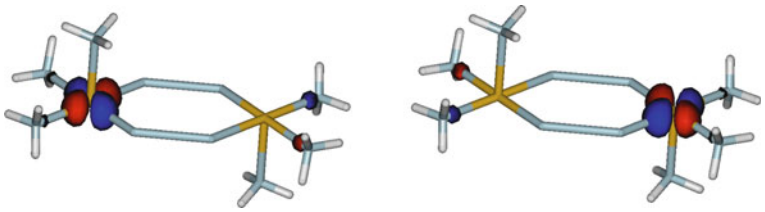

Fig. 5.2 *Left* and *right* localized magnetic orbitals

the CAS Hamiltonian matrix can be written as

$$\begin{array}{c|cccc} & |a\bar{b}\rangle & |b\bar{a}\rangle & |a\bar{a}\rangle & |b\bar{b}\rangle \\ \hline \langle a\bar{b}| & 0 & K_{ab} & t_{ab} & t_{ab} \\ \langle b\bar{a}| & K_{ab} & 0 & t_{ab} & t_{ab} \\ \langle a\bar{a}| & t_{ab} & t_{ab} & U & K_{ab} \\ \langle b\bar{b}| & t_{ab} & t_{ab} & K_{ab} & U \end{array} \tag{5.4}$$

Here $E_{ref} = h_{aa} + h_{bb} + J_{ab}$ is the reference energy and has been subtracted from all diagonal matrix elements. K_{ab} is the direct exchange, U is the on-site repulsion parameter and t_{ab} is the hopping integral and gives a measure of the probability for the electron hopping from site a to b and *vice-versa*.

5.2 Express the energy of the ionic determinants $|a\bar{a}|$ and $|b\bar{b}|$ in terms of the one-electron integrals h and the Coulomb and exchange integrals J and K. What assumption has been made to reduce the diagonal element of these determinants to U?

The diagonalization of the 4×4 matrix gives four eigenvectors, equivalent to those listed above but expressed in local orbitals

$$\begin{aligned} S_g &= \lambda\big(|a\bar{b}| + |b\bar{a}|\big)/\sqrt{2} - \mu\big(|a\bar{a}| + |b\bar{b}|\big)/\sqrt{2} \\ S'_g &= \mu\big(|a\bar{b}| + |b\bar{a}|\big)/\sqrt{2} + \lambda\big(|a\bar{a}| + |b\bar{b}|\big)/\sqrt{2} \\ T_u &= \big(|a\bar{b}| - |b\bar{a}|\big)/\sqrt{2} \\ S_u &= \big(|a\bar{a}| - |b\bar{b}|\big)/\sqrt{2} \end{aligned} \tag{5.5}$$

with energy eigenvalues

$$E(S_g) = K_{ab} + \frac{U - \sqrt{U^2 + 16t_{ab}^2}}{2}$$

$$
\begin{aligned}
E(S'_g) &= K_{ab} + \frac{U + \sqrt{U^2 + 16t_{ab}^2}}{2} \\
E(T_u) &= -K_{ab} \\
E(S_u) &= U - K_{ab}
\end{aligned}
\tag{5.6}
$$

This gives direct access to an analytical expression of J in terms of the previously defined electronic structure parameters

$$
J = E(S_g) - E_T = 2K_{ab} + \frac{U - \sqrt{U^2 + 16t_{ab}^2}}{2} \tag{5.7}
$$

To simplify this expression we use the Taylor expansion $\sqrt{p+q} = \sqrt{p} + \frac{1}{2}q/\sqrt{p} + \cdots$ with $p \gg q$.

$$
J = 2K_{ab} - \frac{4t_{ab}^2}{U} \tag{5.8}
$$

in which one can easily recognize the ferromagnetic ($2K_{ab}$) and antiferromagnetic ($4t_{ab}^2/U$) contributions of the qualitative Kahn–Briat and Hay–Thibeault–Hoffmann models.

5.3 Use the Taylor expansion $\sqrt{p+q} = \sqrt{p} + \frac{1}{2}q/\sqrt{p} + \cdots$ with $p = U^2$ and $q = 16t_{ab}^2$ to derive the simplified expression for J.

A pictorial understanding of this expression can be obtained within a QDPT reasoning using a model space limited to neutral determinants only. Figure 5.3 shows the two determinants $\Phi_I = |a\overline{b}|$ (left) and $\Phi_J = |\overline{a}b|$ on the right. The Heisenberg Hamiltonan matrix element of these two determinants is equal to $-\frac{1}{2}J$, see Eq. 3.34. The arrow connecting the determinants indicates the direct interaction between the determinants parametrized by the direct exchange K_{ab}.

$$
\langle \Phi_I | \hat{H} | \Phi_J \rangle = -\langle a\overline{b} | \hat{H} | b\overline{a} \rangle = -K_{ab} \tag{5.9}
$$

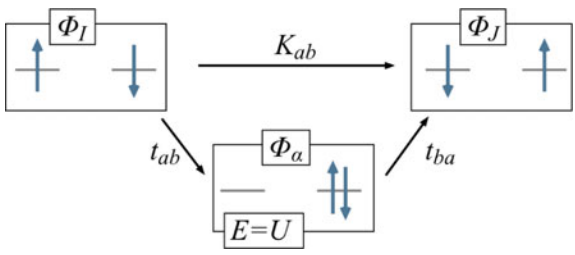

Fig. 5.3 Schematic representation of the interaction between the neutral determinants Φ_I and Φ_J by direct exchange and indirect interaction via ionic determinants

There is, however, also an indirect interaction between the two determinants via the ionic determinants $|a\overline{a}|$ and $|b\overline{b}|$ as shown in the lower part of the figure. Going from left to right, in the first step an electron is transferred from orbital a to orbital b to produce an ionic determinant at energy U with respect to the initial neutral determinant, and in the subsequent step the spin-down electron hops to orbital a to produce $|b\overline{a}|$. The interaction along this path is described with the second-order QDPT expression

$$\frac{\langle \Phi_I|\hat{H}|\Phi_\alpha\rangle\langle\Phi_\alpha|\hat{H}|\Phi_J\rangle}{E_J - E_\alpha} = \frac{\langle a\overline{b}|\hat{H}|b\overline{b}\rangle\langle b\overline{b}|\hat{H}|\overline{a}b\rangle}{0-U} = \frac{-\langle a\overline{b}|\hat{H}|b\overline{b}\rangle\langle b\overline{b}|\hat{H}|b\overline{a}\rangle}{-U} = \frac{t_{ab}\cdot t_{ba}}{U} = \frac{t_{ab}^2}{U} \tag{5.10}$$

where Φ_I, Φ_α and Φ_J are defined in Fig. 5.3. Realizing that there is another indirect path connecting the neutral determinants and adding the direct interaction, we arrive at the following expression

$$\langle \Phi_I|\hat{H}^{eff}|\Phi_J\rangle = -K_{ab} + 2\frac{t_{ab}^2}{U} \tag{5.11}$$

If we compare this to the matrix element of $|a\overline{b}|$ and $|\overline{a}b|$ of the Heisenberg Hamiltonian in Eq. 3.34, we obtain the same expression for J as derived from the diagonalization of the CAS given in Eq. 5.8.

5.4 The above described path can be denoted as $|a\overline{b}| \xrightarrow{t_{ab}} |b\overline{b}| \xrightarrow{t_{ba}} |b\overline{a}|$. Find the other path that connects the two neutral determinants via an ionic determinant.

As long as the variational space is restricted to the metal basis functions, the hopping parameter t_{ab} is extremely small due to the fact that orbitals a and b are strongly localized in different regions of space. Therefore, the antiferromagnetic contribution to J remains small and new mechanisms have to be introduced to describe the coupling. An important improvement is obtained when the role of the bridging ligand is taken into account as schematically represented in Fig. 5.4. Orbitals a and b are again the strongly localized metal orbitals and orbital h is localized on the bridge. In the first step, an electron is transferred from the ligand orbital h to site b, immediately followed by the movement of the electron on site a to the ligand, which creates the ionic determinant $|b\overline{b}|$. To arrive at the neutral determinant with inverted spins with respect to the initial determinant, a beta spin electron is transferred from the ligand to site a and the resulting hole is filled by the beta spin electron that resides on center b. This indirect interaction between the two neutral determinants involves three determinants outside the model space and hence the importance cannot be estimated by second-order QDPT. Instead, one has to apply fourth-order perturbation theory.

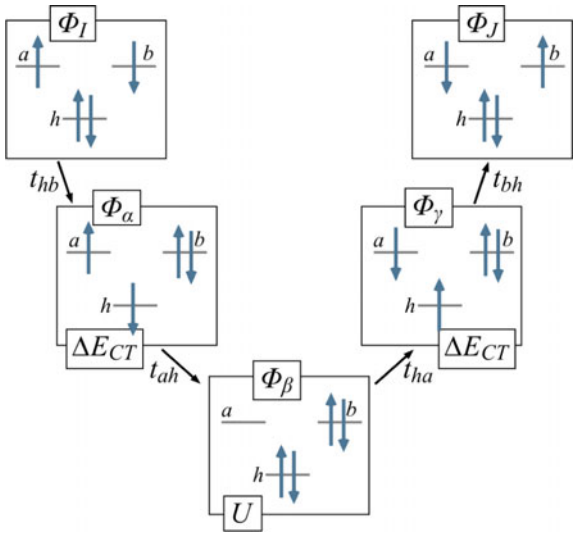

Fig. 5.4 Schematic representation of the interaction between the neutral determinants Φ_I and Φ_J through the bridging ligand

The full expression for the correction at fourth order is rather lengthy, but there is one term that exactly fits on the scheme of Fig. 5.4.

$$E^{(4)} = \cdots + \sum_{\alpha\notin S}\sum_{\beta\notin S}\sum_{\gamma\notin S} \frac{\langle\Phi_I|\hat{H}|\Phi_\alpha\rangle\langle\Phi_\alpha|\hat{H}|\Phi_\beta\rangle\langle\Phi_\beta|\hat{H}|\Phi_\gamma\rangle\langle\Phi_\gamma|\hat{H}|\Phi_J\rangle}{(E_J^{(0)} - E_\alpha^{(0)})(E_J^{(0)} - E_\beta^{(0)})(E_J^{(0)} - E_\gamma^{(0)})} + \ldots \tag{5.12}$$

After replacing the matrix elements in the numerator by the corresponding hopping parameters[1] and the relative energies of the external determinants in the denominator, we obtain a contribution that reads

$$\frac{t_{hb}\cdot t_{ah}\cdot t_{ha}\cdot -t_{bh}}{(0-\Delta E_{CT})(0-U)(0-\Delta E_{CT})} = \frac{t_{ah}^2 t_{bh}^2}{\Delta E_{CT}^2 U} \tag{5.13}$$

An identical expression if obtained for the pathway that starts with the electron hopping from h to a, and hence, the perturbative estimate has to be multiplied by two to obtain the QDPT expression of the matrix element between Φ_I and Φ_J with fourth-order corrections

$$\langle\Phi_I|\hat{H}|\Phi_J\rangle = -K_{ab} + 2\frac{t_{ab}^2}{U} + \frac{2t_{ah}^2 t_{bh}^2}{\Delta E_{CT}^2 U} \tag{5.14}$$

[1] $\Phi_I = |h\bar{h}a\bar{b}| \xrightarrow{t_{hb}} |b\bar{h}a\bar{b}| \xrightarrow{t_{ah}} |b\bar{h}h\bar{b}| \xrightarrow{t_{ha}} |b\bar{a}h\bar{b}| \xrightarrow{t_{bh}} |b\bar{a}h\bar{h}|$. A minus sign appears in the last step when the determinant is written as it appears in the model Hamiltonian $|h\bar{h}\bar{a}b| = \Phi_J$.

Now we replace the bare hopping matrix elements t_{ha} and t_{hb} by an effective parameter through

$$\frac{t_{ha}t_{hb}}{\Delta E_{CT}} = t_{ab}^{eff} \tag{5.15}$$

and arrive at an analytical expression for J using Eq. 3.34

$$J = 2K_{ab} - \frac{4(t_{ab}^{eff})^2}{U} \tag{5.16}$$

where the effect of the bare hopping parameter t_{ab} has been neglected being much smaller than t_{ab}^{eff}, which involves the bridging ligand(s). Note the similarity with the second-order expression of Eq. 5.11. The second, antiferromagnetic term is generally known as the kinetic exchange and is conceptually closely related to the superexchange of Anderson discussed at the end of Sect. 3.1.

5.5 Make a perturbative estimate of the contribution to J of the double LMCT configuration with an energy of ΔE_{2CT}

Putting these concepts to the numerical proof can be done by performing a CASCI calculation with triplet optimized orbitals. Instead of the strongly localized orbitals used in the conceptual reasoning, the optimal orbitals have important delocalization tails on the ligands, as shown in Fig. 5.5. These delocalization tails are just another representation of the through-ligand interaction discussed above, which is easily demonstrated by substituting the definition of the active orbitals with tails on the ligand

$$g = c_1(a + b) + c_2h \qquad \text{and} \qquad u = c_3(a - b) + c_4h' \tag{5.17}$$

into the expression of the lowest singlet state given in Eq. 5.2.

$$\begin{aligned} S_g = \lambda|(c_1(a + b) + c_2h)(c_1(\overline{a} + \overline{b}) + c_2\overline{h})| \\ + \mu|(c_3(a - b) + c_4h')(c_3(\overline{a} - \overline{b}) + c_4\overline{h'})| \end{aligned} \tag{5.18}$$

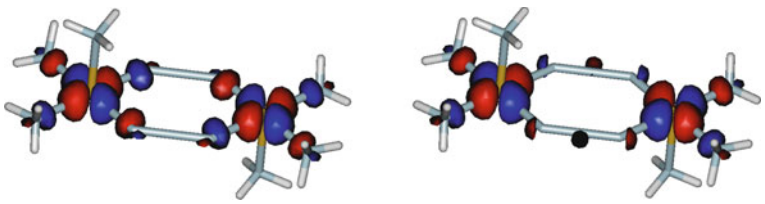

Fig. 5.5 Magnetic orbitals of *gerade* (*left*) and *ungerade* (*right*) symmetry with important delocalization tails on the ligands

Table 5.1 Decomposition of the CAS(2,2) magnetic coupling in the binuclear Cu^{2+} complex with a double azido bridge

Direct exchange	12
t_{ab}^{eff}	−2218
U	20.8×10^4 (=25.8 eV)
Kinetic exchange	−94
$J\big(\mathrm{CAS}(2,2)\big)$	$-82\ \mathrm{cm}^{-1}$

Numbers are given in cm^{-1}

Apart from the previously seen neutral and ionic determinants $|a\bar{b}|$, $|b\bar{a}|$,$|a\bar{a}|$,$|b\bar{b}|$, other determinants such as such as $|h\bar{a}|$, $|b\bar{h}|$, etc. appear in the wave function involving ligand-to-metal charge transfer (LMCT) excitations that were shown to play an important role in the QDPT analysis of the coupling.

The results of the CAS calculation are listed in Table 5.1 and show how the kinetic exchange strongly dominates over the direct exchange, which is rather small as expected from the large distance between the Cu ions. The parameters are directly extracted by comparing the numerical values of the CASCI matrix with the symbolic representation given in Eq. 5.4. The choice for cm^{-1} as energy unit leads to big numbers for U, which is therefore often expressed in eV. The kinetic exchange contribution is calculated from t_{ab}^{eff} and U applying Eq. 5.16: $(-4\cdot(-2218)^2/20800)$.

5.1.2 Beyond the Valence Space

It is obvious that this cannot be the whole story. The calculated magnetic coupling of the Cu^{2+} complex is just 10 % of the experimental and DDCI values. Hence, it is unavoidable to go beyond this valence-only description and incorporate more physical mechanisms in the description.

The 1h, 1p, 1h-1p excitations: In the first step towards the full DDCI result, we analyze the role of the $1h$, $1p$ and $1h$-$1p$ determinants as illustrated in Fig. 5.6. The determinants on the left are pure single excitations and those on the right are single excitations combined with an excitation within the CAS. Because of the Brillouin theorem the contributions of the pure single excitations are strictly zero for the spin state for which the orbitals have been optimized and tiny contributions are observed for the other spin states given that the optimal orbitals for the different spin states are in principle very similar.

The situation is quite different for the single excitations that are combined with electron replacements in the CAS. The $1h$-$1p$ excitation in the determinants marked as *spin polarization* not only excites one of the electrons from orbital h to orbital p but also changes the spin of the excited electron. These so-called triplet excitations have to be compensated by a simultaneous spin change in the active space to maintain the spin of the electronic state under consideration. This gives rise to a triplet coupled

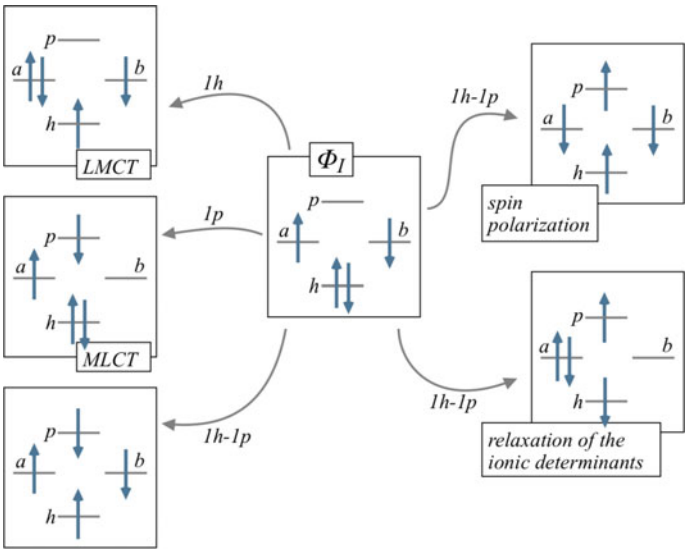

Fig. 5.6 Schematic representation of the $1h$, $1p$ and $1h$-$1p$ determinants. The *left column* shows the pure single excitations, and the *right* the single excitations combined with a change in the occupation of the active orbitals. h and p are assumed to be ligand orbitals, LMCT = ligand-to-metal charge transfer, MLCT = metal-to-ligand charge transfer

electron pair a-b in the active space, from which triplet and singlet spin polarization determinants can be formed through the coupling with the h-p triplet coupled electron pair. The resulting determinants strongly interact both with S_g and T_u (see Eq. 5.5) via the neutral determinants of the reference wave functions, but the matrix element with the ionic determinants is zero since there are more than two differences in the orbital occupancies. The spin polarization introduces spin density on the ligand, which is opposite to the spin density on the metal centers. It can contribute both ferro- and antiferromagnetically depending on the structure of the complex, but it is general more important when the $1h$-$1p$ triplet excitation on the ligand is low in energy, as in conjugated bridges.

5.6 The h-p and the a-b electron pairs are triplet coupled (S = 1) in the determinants that cause spin polarization in the ligands. Which values can be assigned to the total spin by coupling the two S = 1 electron pairs? Are all spin states relevant to the binuclear Cu^{2+} system under study?

The second type of important $1h$-$1p$ determinants combines a spin-conserving h to p excitation with an electron replacement from a to b (or *vice versa*) in the active space. The resulting determinants can be considered as single excitations with respect to the ionic determinants, but Brillouin's theorem does not apply because

the orbitals are not optimized for this ionic charge distribution but rather for the neutral situation. Hence, there is a strong interaction of these determinants with the $|a\overline{a}|$ and $|b\overline{b}|$ determinants, while the interaction with the neutral determinants is much weaker. Since, the ionic determinants are only present in the reference wave function of the S_g state, the addition to the wave function of these $1h$-$1p$ excitations leads to a significant stabilization of the singlet with respect to the triplet state, and consequently, an increase of the antiferromagnetic character of the coupling. Adding single excitations to a determinant that is not expressed in its optimal orbitals is a very efficient way to improve the orbitals. Therefore, this class of $1h$-$1p$ excitations is often interpreted as relaxing the ionic determinants in the wave function, lowering their energy with respect to the neutral determinants, that is, a decrease of U. In line with the expression for J given in Eq. 5.16, a smaller U makes the kinetic exchange more effective and J more antiferromagnetic.

The total effect of the single excitations is a large step in the right direction, both spin polarization and the relaxation of the ionic determinants cause antiferromagnetic contributions, but still the value of the coupling is only ∼50 % of the final value and other mechanisms have to be included.

5.7 Assuming that the $1h$-$1p$ excitations do not affect the hopping parameter t_{ab}^{eff}, calculate the energy lowering effect on U of the inclusion of the $1h$-$1p$ excitations combined with the electron replacement in the active space using the numerical data from Tables 5.1 and 5.2.

The last step: 2h, 2p, 2h-1p and 1h-2p excitations. The double excitations of the $2h$ and $2p$ class (shown in the left column of Fig. 5.7) only contribute very little to the magnetic coupling of the two Cu ions. They correspond to double ligand-to-metal or metal-to-ligand charge transfer excitations, respectively. The weak interaction is largely explained by the high energy of these determinants with respect to the neutral determinants. This energy difference enters the denominator of the perturbative expression of the effect of the external determinants, and hence, higher-lying determinants contribute less to J.

Table 5.2 Decomposition of the DDCI magnetic coupling in the binuclear Cu^{2+} complex with a double azido bridge

Direct exchange	12
Kinetic exchange	−94
Spin polarization	−59
Relaxation of the ionic determinants	−221
Double CT	−13
Relaxation of the CT determinants	−427
J	−802 cm^{-1}

Numbers are given in cm^{-1}

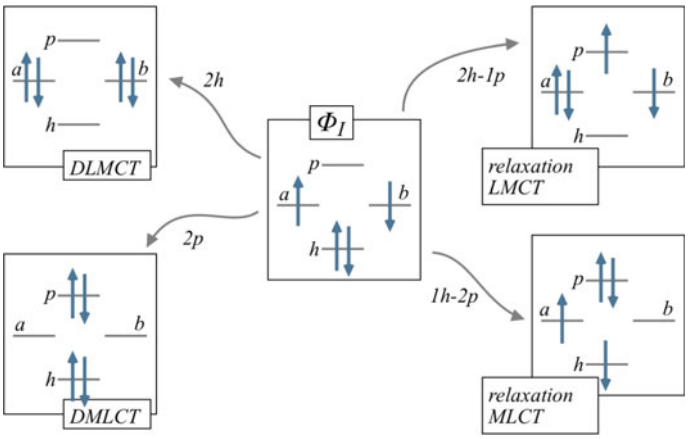

Fig. 5.7 Schematic representation of the $2h$, $2p$, $2h$-$1p$ and $1h$-$2p$ determinants. DLMCT = double ligand-to-metal charge transfer, DMLCT = double metal-to-ligand charge transfer

The single excitation connected to the ligand-to-metal charge transfer process does not interact with the reference wave function by Brillouin's theorem. However, the combination of a LMCT excitation with a single excitation from occupied to virtual orbitals ($1h + 1h$-$1p = 2h$-$1p$) gives rise to a relaxation process similar to the one described before for the ionic determinants, right column of Fig. 5.7. The addition of the relaxed LMCT determinants to the CI wave function has a large impact on the singlet-triplet splitting and virtually always favors the antiferromagnetic character of the coupling. Analogously, the $1h$-$2p$ excitations can be considered to introduce the relaxation of the metal-to-ligand charge transfer excitations. The addition of these determinants is ferromagnetic in most cases, but usually smaller than the effect of the $2h$-$1p$ determinants. Hence the net effect of these double excitations is a significant increase of the singlet-triplet gap as can be seen in Table 5.2. The $2h$ and $2p$ determinants give a tiny contribution to J, but the inclusion of the $2h$-$1p$ and $1h$-$2p$ determinants brings the computational estimate of J in close agreement with the experimental value.

Remember that inclusion of the largest group of determinants that can interact with the neutral determinants, the $2h$-$2p$ determinants, has a negligible effect on the energy difference and is not included in the DDCI wave function and not considered in the analysis of the mechanism of the coupling. This will be numerically shown for our example compound in the next section.

5.1.3 Decomposition with MRPT2

A similar exercise can be performed based on the results of a MRPT2 calculation with a CAS(2,2) reference wave function. Both NEVPT2 and CASPT2 distinguish the contributions to the second-order energy correction of the different excitation classes

Table 5.3 Decomposition of the CASPT2 contribution to the magnetic coupling in the binuclear Cu^{2+} complex with a double azido bridge

Excitation class	$E^{(2)}$(singlet)	$E^{(2)}$(triplet)	Difference
$1h$	0.000000	0.000000	0.0
$1p$	0.000000	0.000000	0.0
$1h$-$1p$	−0.017278	−0.018653	−301.8
$2h$	−0.000010	−0.000027	−3.9
$2p$	−0.000011	−0.000031	−4.4
$2h$-$1p$	−0.095270	−0.095938	−144.6
$1h$-$2p$	−0.213555	−0.213649	−20.8
$2h$-$2p$	−3.654102	−3.653976	27.5
CASPT2	−3.980233	−3.982275	−448.1[a]

Energies are given in Hartree, the difference in cm^{-1}

[a]The total magnetic coupling $J = J[\text{CAS}(2,2)] + \text{CASPT2} = -101.4 + -448.1 = -549.5\ cm^{-1}$

as exemplified in Table 4.1. The analysis is completely straightforward, one just has to subtract the energy contributions of the different spin states in a class-by-class manner to decompose the magnetic coupling. Table 5.3 shows the contribution of the different excitation classes in the example compound studied above with DDCI.

There are two major contributions to the energy difference of singlet and triplet. In the first place, the $1h$-$1p$ excitations, which cause spin polarization and relaxation of the ionic determinants. Unfortunately, it is not possible to separate the two contributions as in DDCI. The second large contribution arises from the $2h$-$1p$ excitations, which also enhances the singlet stability, as expected. The $2h$ and $2p$ excitations are nearly zero and the $1h$-$2p$ class also gives a rather small contribution for the present system. The total contribution of the $2h$-$2p$ class is by far the largest, it constitutes approximately 92 % of $E^{(2)}$, but the differential effect is very small. The non-zero contribution to the difference may seem surprising given the fact that the justification of DDCI is based on the zero contribution of these excitations at second-order perturbation theory. However, this reasoning is based on a common orbital basis for the spin states, which is not used in the CASPT2 calculation. It is common practice to optimize the orbitals for each spin state separately, contrary to MRCI where normally one set of orbitals is used. The use of state-specific orbitals also explains the strictly zero contribution of the $1h$ and $1p$ excitations for both states.

5.2 Mapping Back on a Valence-Only Model

The preceding section shows that a valence-only description of the coupling leads to rather poor predictions. Although the sign of the coupling is often (but not always) correctly reproduced, it can be stated that the strength of the coupling is underestimated by at least one order of magnitude. This is in sharp contrast with the success of

the qualitative valence models discussed in Chap. 4, which are capable of explaining many magnetostructural correlations and rationalize the relative size of J in large families of compounds. These models seem to contain all the essential physics but their parametrization with *ab initio* calculations is deficient. Hence, it may be advantageous to construct a simple valence-only picture in which the values of the parameters t_{ab}, U and K_{ab} are replaced by effective values that absorb all the effects discussed above that go beyond the valence-only description. In fact, we have already seen how the bare hopping parameter t_{ab} was replaced by an effective t_{ab} due to the partial delocalization of the magnetic orbitals onto the ligands upon the change from strongly localized orbitals to self-consistently optimized molecular orbitals as schematically illustrated in Fig. 5.8.

A rigorous way to construct a valence-only model with *ab initio* methods is to make use of the effective Hamiltonian theory presented in Chap. 1. First, we define the basis of the model space as $\{|a\bar{b}|, |b\bar{a}|, |a\bar{a}|, |b\bar{b}|\}$ and use the matrix of Eq. 5.4 to represent the effective Hamiltonian. Then we replace the bare parameters obtained in a valence-only *ab initio* calculation with effective parameters that include all the effects that have been discussed in the previous section. This is done by selecting those four roots from the *ab initio* calculation that have the largest projection on the model space. After orthogonalization and normalization, Eq. 1.90 or 1.92 is used to construct a numerical Hamiltonian from which the new, effective parameters can be extracted by the comparison with Eq. 5.4.

To numerically illustrate the procedure, we will treat the magnetic coupling of two Cu^{2+} ions in the previously introduced $SrCu_2O_3$ compound with Cu_2O_3 layers separated by Sr^{2+} ions (see Sect. 3.4.2). We recall that the copper ions form a regular pattern that can best be described as a ladder structure as depicted in Fig. 5.9. Among

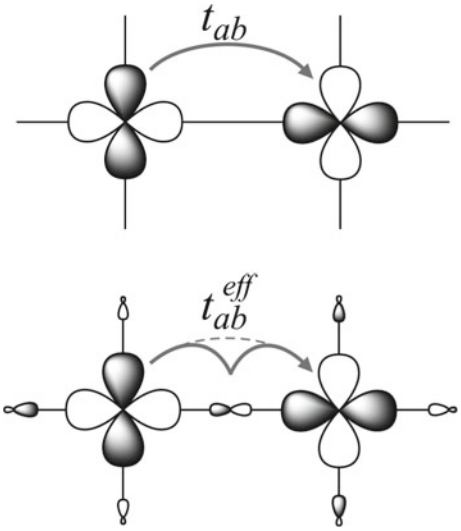

Fig. 5.8 *Top* direct (through space) hopping between two magnetic centers by t_{ab} with strongly localized atomic orbitals; *Bottom* effective (through ligand) hopping by t_{ab}^{eff} with self-consistently optimized magnetic orbitals, which have delocalization tails on the (bridging) ligands

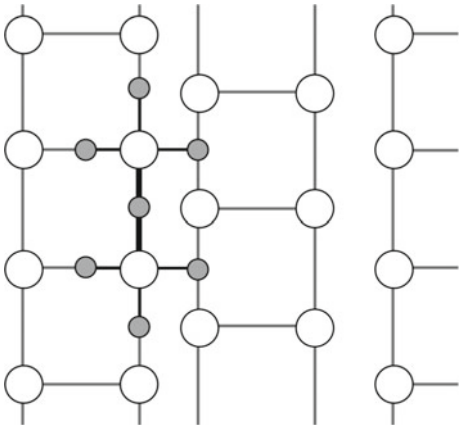

Fig. 5.9 Ladder-like structure of $SrCu_2O_3$. The *open circles* represent Cu^{2+} ions, the small *grey circles* are oxygens, only the oxygens belonging to the Cu_2O_7 cluster are shown. The Sr ions are below and above this plane

the sixteen lowest roots of a DDCI calculation on an embedded Cu_2O_7 cluster (see Sect. 6.3.1), the roots 1, 2, 7 and 8

$$\begin{aligned}
\Psi_1 &= -0.9224\big(|a\bar{b}| + |b\bar{a}|\big) - 0.1223\big(|a\bar{a}| + |b\bar{b}|\big) + \cdots \\
\Psi_2 &= -0.6626\big(|a\bar{b}| - |b\bar{a}|\big) + \cdots \\
\Psi_7 &= 0.4159\big(|a\bar{a}| - |b\bar{b}|\big) + \cdots \\
\Psi_8 &= 0.1704\big(|a\bar{b}| + |b\bar{a}|\big) - 0.5324\big(|a\bar{a}| + |b\bar{b}|\big)
\end{aligned} \tag{5.19}$$

have the largest norm after projection on the model space. The normalized projections, denoted $\widetilde{\Psi}'_1 \ldots \widetilde{\Psi}'_4$, will be used for the construction of the effective Hamiltonian. The relative energies are 0.000, 0.158, 6.489 and 6.547 eV, respectively. The Bloch effective Hamiltonian uses biorthogonal vectors, which are obtained from Eq. 5.19 by

$$\begin{aligned}
\widetilde{\Psi}'^{\dagger}_1 &= \frac{1}{\sqrt{1-s^2}}\big(\widetilde{\Psi}'_1 - s\widetilde{\Psi}'_4\big) = -0.9524\big(|a\bar{b}| + |b\bar{a}|\big) - 0.3048\big(|a\bar{a}| + |b\bar{b}|\big) \\
\widetilde{\Psi}'^{\dagger}_2 &= \widetilde{\Psi}'_2 = \big(|a\bar{b}| - |b\bar{a}|\big)/\sqrt{2} \\
\widetilde{\Psi}'^{\dagger}_3 &= \widetilde{\Psi}'_3 = \big(|a\bar{a}| - |b\bar{b}|\big)/\sqrt{2} \\
\widetilde{\Psi}'^{\dagger}_4 &= \frac{1}{\sqrt{1-s^2}}\big(-s\widetilde{\Psi}'_1 + \widetilde{\Psi}'_4\big) = 0.1315\big(|a\bar{b}| + |b\bar{a}|\big) - 0.9913\big(|a\bar{a}| + |b\bar{b}|\big)
\end{aligned} \tag{5.20}$$

where $s = \langle\widetilde{\Psi}'_1|\widetilde{\Psi}'_4\rangle$.

Table 5.4 Electronic structure parameters of a valence-only model for the magnetic interactions between two Cu^{2+} ions in $SrCu_2O_3$

	$\hat{H}^{eff}$	K_{ab}^{eff}	U^{eff}	t_{ab}^{eff}	J_{pert}
Valence-only	CASCI	16	24.6	−617	−30
Dressed model	Bloch	55	6.0	−1005/−417	−227
	Gram-Schmidt	−22	6.3	−427	−160

U is given in eV, the other parameters in meV. J_{pert} is calculated using Eq. 5.8. The magnetic coupling extracted from the DDCI energies of the lowest singlet and triplet states is −158 meV. The dressed models are extracted from DDCI calculations using triplet orbitals

5.8 Calculate the norm of the projections of Ψ_i on the model space and give the expressions of $\widetilde{\Psi}'_{1,4}$. Are all $\widetilde{\Psi}'_i$ mutually orthogonal? Check that the biorthogonal vectors $\widetilde{\Psi}_i^{\dagger}$ fulfill the orthogonality properties of Eq. 1.89.

Now we apply the Bloch formula (Eq. 1.90) to construct the effective Hamiltonian. The resulting parameters are given in the second line of Table 5.4 together with an estimate of J from the sum of the direct and kinetic exchange given in Eq. 5.8. As most particular results, we see that U is strongly reduced in comparison to the valence-only value (CASCI) and that the non-hermiticity is manifest in the two different values of the hopping parameter: $t_1 = \langle a\overline{b}|\hat{H}^{eff}|a\overline{a}\rangle$ and $t_2 = \langle a\overline{a}|\hat{H}^{eff}|a\overline{b}\rangle$.

The Gram–Schmidt procedure provides a simpler orthogonalization scheme that leads to a hermitian effective Hamiltonian. Since $\widetilde{\Psi}'_2$ and $\widetilde{\Psi}'_3$ are already orthogonal to the other projections, we only have to worry about $\widetilde{\Psi}'_1$ and $\widetilde{\Psi}'_4$. This means that the coefficients of $\widetilde{\Psi}_4^{\perp}$ are defined by $\widetilde{\Psi}'_1$, that is, if $\widetilde{\Psi}'_1 = \alpha\big(|a\overline{b}| + |b\overline{a}|\big) + \beta\big(|a\overline{a}| + |b\overline{b}|\big)$ then the orthogonal counterpart $\widetilde{\Psi}_4^{\perp} = -\beta\big(|a\overline{b}| + |b\overline{a}|\big) + \alpha\big(|a\overline{a}| + |b\overline{b}|\big)$, independent of the shape of Ψ_4 and only the energy of this state is used in the construction of $\hat{H}^{eff}$. The parameters extracted with the Gram-Schmidt orthogonalized vectors are listed in the third row of the table and reveal besides the expected large decrease of U, a negative effective direct exchange and, by construction, a hermitian form with only one estimate for t. The estimate of J based on Eq. 5.8 is in excellent agreement with the result of the full DDCI calculation.

The observed changes suffered by the parameters upon dressing them with the effects that go beyond the valence space can at least partially be rationalized by looking at the interaction of the model space determinants with those in the external space. The interaction of the spin-conserving $1h$-$1p$ excitations with the neutral determinants is (nearly) zero due to Brillouin's theorem. On the contrary, the interaction with the ionic determinants is strong (see the right part of Fig. 5.10). Hence, this class of external determinants largely decreases the on-site repulsion U as previously seen in Exercise 6.7 and confirmed here in the example.

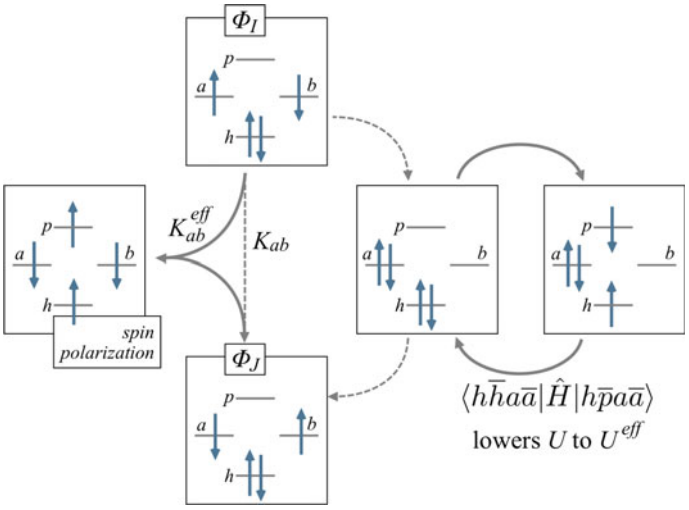

Fig. 5.10 Effect of the spin-conserving (*right*) and non spin-conserving (*left*) $1h$-$1p$ determinants on the on-site repulsion U and the direct exchange parameter K_{ab}. The interactions in a valence-only treatment are marked with *dashed lines*

The non spin-conserving excitations (the spin polarization) simultaneously interact with both neutral determinants:

$$\langle h\bar{h}a\bar{b}|\hat{H}|h\bar{a}\,p\bar{b}\rangle\langle h\bar{a}\,p\bar{b}|\hat{H}|h\bar{h}b\bar{a}\rangle \neq 0 \tag{5.21}$$

and hence, turns the direct exchange parameter $K_{ab} = \langle a\bar{b}|\hat{H}|b\bar{a}\rangle$ into an effective parameter that parametrizes the direct exchange dressed with spin polarization effects. Since this latter effect can be antiferromagnetic in nature, the apparent counterintuitive situation may arise that K_{ab}^{eff} turns out to be negative, whereas the bare K_{ab} is positive by definition.

Finally, t_{ab} is expected to be influenced by the $2h$-$1p$ excitations, which can be seen as a LMCT excitation ($1h$) coupled to a single excitation from an occupied to a virtual orbital ($1h$-$1p$) that relaxes the LMCT configuration. This should lead to an increase of the hopping between the magnetic centers. It is, however, difficult to isolate the effect of the $2h$-$1p$ excitations [4] due to the occurrence of interactions with other excited determinants and the interference of the $1h$-$2p$ excitations. Therefore, the hopping parameter t_{ab}^{eff} turns out to be somewhat smaller than the bare value. Experience has shown that t does not suffer dramatic changes when electron correlation is included in the valence-only models.

5.3 Analysis with Single Determinant Methods

The multiconfigurational wave function is a natural starting point for a decomposition of the magnetic coupling in polynuclear complexes. The relative magnitude of the coefficients of the determinants gives a straightforward strategy to analyze the importance of the different mechanisms. The disadvantage of this approach is of course the rather heavy computational burden, which limits the applicability to medium-sized systems. Alternatively, DFT can be used for larger systems but the analysis of the results cannot be made in the same way as discussed above, since there is only one Slater determinant that contains all the physics. Instead, one can decompose the coupling by a series of partial orbital optimizations of the high-spin and broken symmetry determinants [5]. The intermediate energy differences can be related to the direct and kinetic exchange, and the spin polarization as will be shown below.

The analysis starts with a restricted open-shell Kohn-Sham (ROKS) calculation on the HS state. If necessary, the magnetic orbitals are transformed to the representation with local orthogonal orbitals a and b, as shown in the first column of Fig. 5.11. Staying within the spin-restricted formalism makes that for each α orbital a β orbital can be found which has the same spatial part. In the first step, the direct exchange is estimated from the energy difference of the HS(ROKS) and a BS determinant in which only the spin of one of the unpaired electrons is inverted, but neither the *core* nor the magnetic orbitals are optimized.

$$E(\text{BS-ROKS}) = E(\text{HS-ROKS}) + K_{ab} \tag{5.22}$$

With the help of Yamaguchi's expression (Eq. 4.65), one can define the direct exchange contribution (J_{DE}) to the total magnetic coupling as

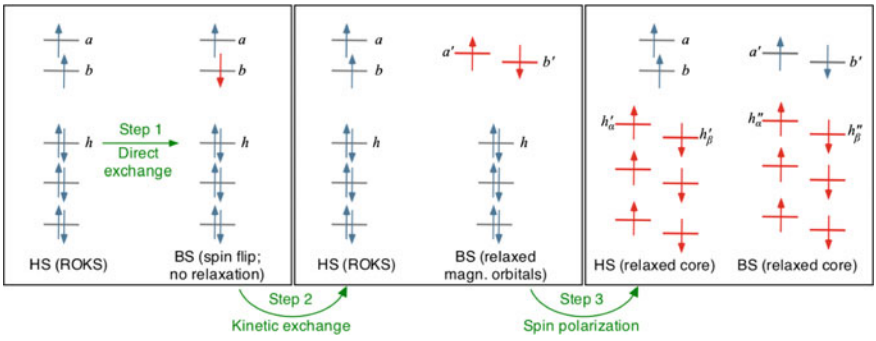

Fig. 5.11 Schematic representation of the decomposition of the magnetic coupling for computational schemes based on a single determinant. The orbitals and electrons marked in *red* are subject to changes with respect to the previous step, the rest is kept frozen

$$J_{DE} = \frac{2\big(E(\text{BS-ROKS}) - E(\text{HS-ROKS})\big)}{\langle \hat{S}^2 \rangle_{\text{HS-ROKS}} - \langle \hat{S}^2 \rangle_{\text{BS-ROKS}}} = \frac{2K_{ab}}{2-1} = 2K_{ab} \tag{5.23}$$

Step 2 consists in the optimization of the magnetic orbitals of the BS determinant in the fixed field of the doubly occupied orbitals, a so-called frozen core (FC). The magnetic orbitals become more delocalized and, more specifically, gain some amplitude on the other magnetic center. This means that the unpaired electrons can move from one center to the other and activate the kinetic exchange mechanism. The contribution to J is

$$J_{KE} = \frac{2\big(E(\text{BS-FC}) - E(\text{HS-ROKS})\big)}{2 - \langle \hat{S}^2 \rangle_{\text{BS-FC}}} - J_{DE} \tag{5.24}$$

To a very good approximation, the spatial part of the new magnetic BS orbitals a' and b' can be written as a weighted sum of the ROKS orbitals

$$a' = (\cos\alpha)a + (\sin\alpha)b \qquad b' = (\sin\alpha)a + (\cos\alpha)b \tag{5.25}$$

5.9 Calculate the overlap of the spatial part of the relaxed magnetic orbitals for $\alpha = 0, \pi/60, \pi/20, \pi/4, \pi/2$.

The interaction with the virtual orbitals is very small and can be neglected for the present analysis purposes. Substituting these expressions in the BS determinant

$$\Phi_{BS} = (\cos\alpha)^2 |a\overline{b}| + (\sin\alpha)^2 |b\overline{a}| + (\sin\alpha\cos\alpha)\big(|a\overline{a}| + |b\overline{b}|\big) \tag{5.26}$$

shows immediately that the relaxation activates the kinetic exchange by introducing the ionic determinants $|a\overline{a}|$ and $|b\overline{b}|$ in the BS determinant. The optimization of a and b makes that the $\hat{S}^2$ expectation value of the BS determinant is not exactly one as for the BS-ROKS determinant (see Problems).

The last step relaxes the core orbitals for the HS and BS determinants, keeping the magnetic orbitals fixed to what was obtained in step 2 (frozen magnetic orbitals: FM). Lifting the restrictions on the spin symmetry in the core orbitals introduces different α and β spin orbitals, and hence, accounts for the spin polarization of the core electrons in response to the parallel (HS) or antiparallel (BS) unpaired electrons. The energy difference between the BS-FM and HS-FM determinants gives access to the spin polarization contribution to J via

$$J_{SP} = \frac{2\big(E(\text{BS-FM}) - E(\text{HS-FM})\big)}{\langle \hat{S}^2 \rangle_{\text{HS-FM}} - \langle \hat{S}^2 \rangle_{\text{BS-FM}}} - J_{DE} - J_{KE} \tag{5.27}$$

The sum of the three contributions is close to the magnetic coupling constant that is obtained in a standard calculation when the Kohn-Sham orbitals are optimized without imposing any restriction on the variational process.

$$J \approx J_{DE} + J_{KE} + J_{SP} \tag{5.28}$$

There is no *a priori* reason to determine the different contributions in this order. Alternatively, the spin polarization can be calculated before relaxing the magnetic orbitals (inverting step 2 and 3) or independently, both taking the orbitals of step 1 as starting point. However, the examples given in Ref. [5] show that the order chosen here gives the smallest deviation from the fully relaxed energy difference, and hence, includes the largest part of the physics.

5.4 Analysis of Complex Interactions

The analysis of the interaction between magnetic moments is not restricted to the isotropic bilinear exchange of two $S = 1/2$ centers but can also be applied to systems with higher spins and more magnetic centers. In this section, we will first decompose the magnetic coupling between two Ni^{2+} ($S = 1$) ions with a sizeable biquadratic exchange to pinpoint the origin of the deviations to the standard Heisenberg Hamiltonian. Secondly, we will focus attention on the four-spin cyclic exchange, and finally, we will describe how these interactions can be estimated within the DFT framework.

5.4.1 Decomposition of the Biquadratic Exchange

One of the central assumptions of the Heisenberg model Hamiltonian is that the local spin states are well separated in energy from excited spin states. We will demonstrate that non-Heisenberg behavior emerges as soon as this is no longer true. The biquadratic exchange is in general a rather small term in the total interaction of the spins in polynuclear TM-3d complexes. There are only a few examples where it is important to include them for obtaining an accurate description of the lowest-energy levels. Returning to the binuclear complexes with a double azido bridge, we will here analyze the magnetic coupling of the Ni^{2+} model complex shown in Fig. 5.12. The interaction of the spins strongly depends on the δ-angle and ranges from approximately 100 cm^{-1} for $\delta = 0°$ to nearly zero for $\delta = 45°$, which is accurately reproduced with DDCI [6]. More interestingly, the singlet, triplet and quintet DDCI energies do not strictly follow the expected Landé pattern, especially for small δ. Deviations up to 3 % are observed and we will use the corresponding wave functions to analyze the origin of the deviations to the standard Heisenberg spacing.

The magnetic orbitals are expressed again in orthogonal atomic-like orbitals, denoted φ_1, φ_2 for the two magnetic orbitals on site A and φ_3, φ_4 for the orbitals on

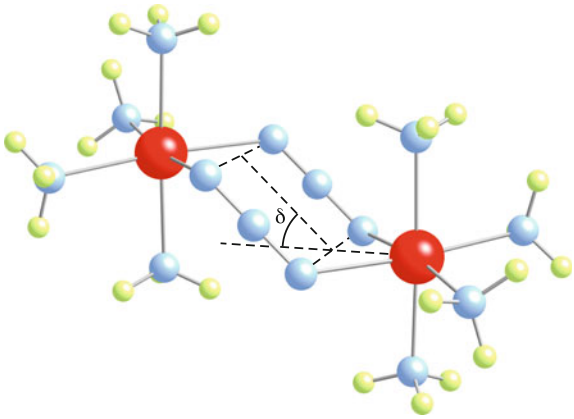

Fig. 5.12 $(NH_3)_3$–Ni–$(\mu$-$N_3)_2$–Ni–$NH_3)_3$ model complex and definition of the angle δ

center B. The local ground state is a triplet denoted as $T_A^{1,0,-1}$ for the three degenerate M_S components on center A and $T_B^{1,0,-1}$ for the components of the triplet on center B.

$$\begin{aligned} T_A^+ &= |\varphi_1\varphi_2| & T_B^+ &= |\varphi_3\varphi_4| \\ T_A^- &= |\overline{\varphi}_1\overline{\varphi}_2| & T_B^- &= |\overline{\varphi}_3\overline{\varphi}_4| \\ T_A^0 &= (|\varphi_1\overline{\varphi}_2| - |\varphi_2\overline{\varphi}_1|)/\sqrt{2} & T_B^0 &= (|\varphi_3\overline{\varphi}_4| - |\varphi_4\overline{\varphi}_3|)/\sqrt{2} \end{aligned} \tag{5.29}$$

Note that the superscript indicates the M_S-value of the function. In addition we also define a local singlet with the same orbital occupancy but a different spin coupling. This CSF dominates the lowest excited singlet state in octahedral Ni^{2+} complexes and will be named here a non-Hund state

$$S_A^0 = (|\varphi_1\overline{\varphi}_2| + |\varphi_2\overline{\varphi}_1|)/\sqrt{2} \qquad S_B^0 = (|\varphi_3\overline{\varphi}_4| + |\varphi_4\overline{\varphi}_3|)/\sqrt{2} \tag{5.30}$$

The total wave functions of the binuclear complex can be constructed from the products of these local functions. In order to find any possible interactions between the lowest singlet, triplet and quintet states and the newly introduced non-Hund singlet, all products are written in their $M_S = 0$ variant.

$$T_A^+ T_B^- = |\varphi_1\varphi_2\overline{\varphi}_3\overline{\varphi}_4| = T^+T^- \tag{5.31}$$

$$T_A^- T_B^+ = |\overline{\varphi}_1\overline{\varphi}_2\varphi_3\varphi_4| = T^-T^+ \tag{5.32}$$

$$\begin{aligned} T_A^0 T_B^0 = \frac{1}{2}\big(|\varphi_1\overline{\varphi}_2| - |\varphi_2\overline{\varphi}_1|\big)\big(|\varphi_3\overline{\varphi}_4| - |\varphi_4\overline{\varphi}_3|\big) = \frac{1}{2}\big(|\varphi_1\overline{\varphi}_2\varphi_3\overline{\varphi}_4| \\ - |\varphi_1\overline{\varphi}_2\varphi_4\overline{\varphi}_3| - |\varphi_2\overline{\varphi}_1\varphi_3\overline{\varphi}_4| + |\varphi_2\overline{\varphi}_1\varphi_4\overline{\varphi}_3|\big) = T^0T^0 \end{aligned} \tag{5.33}$$

$$\begin{aligned} T_A^0 S_B^0 = \frac{1}{2}\big(|\varphi_1\overline{\varphi}_2| + |\varphi_2\overline{\varphi}_1|\big)\big(|\varphi_3\overline{\varphi}_4| - |\varphi_4\overline{\varphi}_3|\big) = \frac{1}{2}\big(|\varphi_1\overline{\varphi}_2\varphi_3\overline{\varphi}_4| \\ + |\varphi_1\overline{\varphi}_2\varphi_4\overline{\varphi}_3| - |\varphi_2\overline{\varphi}_1\varphi_3\overline{\varphi}_4| - |\varphi_2\overline{\varphi}_1\varphi_4\overline{\varphi}_3|\big) = T^0S^0 \end{aligned} \tag{5.34}$$

$$S_A^0 T_B^0 = \frac{1}{2}\left(|\varphi_1\overline{\varphi}_2| + |\varphi_2\overline{\varphi}_1|\right)\left(|\varphi_3\overline{\varphi}_4| - |\varphi_4\overline{\varphi}_3|\right) = \frac{1}{2}\left(|\varphi_1\overline{\varphi}_2\varphi_3\overline{\varphi}_4| - |\varphi_1\overline{\varphi}_2\varphi_4\overline{\varphi}_3| + |\varphi_2\overline{\varphi}_1\varphi_3\overline{\varphi}_4| - |\varphi_2\overline{\varphi}_1\varphi_4\overline{\varphi}_3|\right) = S^0T^0 \tag{5.35}$$

$$S_A^0 S_B^0 = \frac{1}{2}\left(|\varphi_1\overline{\varphi}_2| + |\varphi_2\overline{\varphi}_1|\right)\left(|\varphi_3\overline{\varphi}_4| + |\varphi_4\overline{\varphi}_3|\right) = \frac{1}{2}\left(|\varphi_1\overline{\varphi}_2\varphi_3\overline{\varphi}_4| + |\varphi_1\overline{\varphi}_2\varphi_4\overline{\varphi}_3| + |\varphi_2\overline{\varphi}_1\varphi_3\overline{\varphi}_4| + |\varphi_2\overline{\varphi}_1\varphi_4\overline{\varphi}_3|\right) = S^0S^0 \tag{5.36}$$

These six CSFs can be combined to form spin eigenstates; three states with local triplet coupling on both magnetic centers and three more with at least one magnetic center in a locally excited (non-Hund) state.

$$Q = \sqrt{\frac{2}{3}}\left(T^0T^0 + \frac{1}{2}(T^+T^-)\right) \tag{5.37a}$$

$$T = \frac{1}{\sqrt{2}}\left(T^+T^- - T^-T^+\right) \tag{5.37b}$$

$$S = \frac{1}{\sqrt{3}}\left(T^0T^0 - T^+T^- - T^-T^+\right) \tag{5.37c}$$

$$NH1 = \frac{1}{\sqrt{2}}\left(T^0S^0 + S^0T^0\right) \tag{5.38a}$$

$$NH2 = \frac{1}{\sqrt{2}}\left(T^0S^0 - S^0T^0\right) \tag{5.38b}$$

$$NH3 = S^0S^0 \tag{5.38c}$$

These six CSFs are the basis of the model space of the determinants of the four-electron/four-orbital CAS calculation with the restriction of one electron per orbital. The matrix representation of the model space is

	$\|Q\rangle$	$\|T\rangle$	$\|S\rangle$	$\|NH1\rangle$	$\|NH2\rangle$	$\|NH3\rangle$
$\langle Q\|$	$E_0 - 2K - 2K'$					
$\langle T\|$	0	$E_0 - 2K$				
$\langle S\|$	0	0	$E_0 - 2K + K'$			
$\langle NH1\|$	0	0	0	$E_0 + 2K'$		
$\langle NH2\|$	0	$K_{24} - K_{13}$	0	0	$E_0 + 2K"$	
$\langle NH3\|$	0	0	$\sqrt{3}(K'' - K')$	0	0	$E_0 + 2K - K'$

where E_0 contains all the one-electron terms and the Coulomb integrals. K is the average of the on-site exchange integrals $2K = K_{12} + K_{34}$. K' and K'' are sums of two-center exchange integrals, and hence, much smaller. $2K' = K_{13} + K_{24}$; $2K'' = K_{14} + K_{23}$. The different exchange integrals $K_{ij} = \langle\varphi_i\varphi_j|1/r_{ij}|\varphi_j\varphi_i\rangle$ are defined in Fig. 5.13.

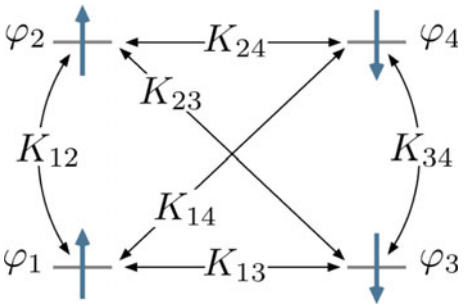

Fig. 5.13 Definition of the exchange integrals that appear in the matrix representation of the model space formed by the neutral determinants of the four-electron/four-orbital case. For the centrosymmetric case here considered $K_{12} = K_{34} \gg K_{13} \approx K_{24} > K_{14} = K_{23}$

In the first place, we recognize that without considering the non-Hund states, there is a strict regular order of the singlet, triplet and quintet states. The triplet-quintet splitting ($2K'$) is twice as large as the energy difference between triplet and singlet. Since this model space only considers the neutral determinants, it is not unexpected that the quintet spin coupling leads to the lowest energy. The non-Hund states with one local singlet (NH1 and NH2) lie at relative energies of approximately $2K$ and the double non-Hund state is found around $4K$ with respect to the Q, T, and S states.

The only non-zero off-diagonal terms in the matrix reveal small interactions between T and $NH2$ and between S and $NH3$. However, these matrix elements are usually very small. The exchange integrals involved are all two-center integrals and therefore rather small. Moreover, the different two-center integrals are similar in magnitude and tend to cancel each other. Obviously, the quintet state cannot have additional contributions from the non-Hund states, since singlet coupling on one of the magnetic centers cannot lead to a state with overall quintet coupling. Although these interactions are at the very origin of the deviations to the regular Landé spacing of the energies, a second ingredient is necessary to activate the contribution of the non-Hund states. The key to a sizeable non-Heisenberg behaviour lies in the interaction of the non-Hund states with the ionic determinants, which in turn interact with the singlet and triplet functions of Eq. 5.37. To illustrate this effect, the model space is enlarged with the eight ionic determinants that interact with the neutral ones defined in Eq. 5.31. The *plus* and *minus* combinations of the ionic determinants give rise to four singlet and four triplet CSFs with three electrons on one center and one electron on the other.

$$I_{1,2} = \left(|\varphi_1\overline{\varphi}_1\varphi_2\overline{\varphi}_4| \pm |\varphi_1\overline{\varphi}_1\varphi_4\overline{\varphi}_2|\right)/\sqrt{2} \tag{5.39a}$$

$$I_{3,4} = \left(|\varphi_3\overline{\varphi}_3\varphi_4\overline{\varphi}_2| \pm |\varphi_3\overline{\varphi}_3\varphi_2\overline{\varphi}_4|\right)/\sqrt{2} \tag{5.39b}$$

$$I_{5,6} = \left(|\varphi_2\overline{\varphi}_2\varphi_1\overline{\varphi}_3| \pm |\varphi_2\overline{\varphi}_2\varphi_3\overline{\varphi}_1|\right)/\sqrt{2} \tag{5.39c}$$

$$I_{7,8} = \left(|\varphi_4\overline{\varphi}_4\varphi_1\overline{\varphi}_3| \pm |\varphi_4\overline{\varphi}_4\varphi_2\overline{\varphi}_1|\right)/\sqrt{2} \tag{5.39d}$$

There are more ionic determinants, e.g. $|\phi_1\overline{\phi}_1\phi_2\overline{\phi}_3|$, but these do not interact with T or S when ϕ_1 and ϕ_3 belong to a different irreducible representation than ϕ_2 and ϕ_4. The use of spin symmetry adapted configurations allows us to write the full 15×15 matrix representation of the model space in three separate blocks. The first one is one-dimensional and only contains the neutral quintet CSF, the second one contains all the triplet CSFs: T, NH2 and the even-numbered I_i CSFs. The third sub-block of the total reference space is formed by the singlets: S, NH3 and the odd-numbered I_i CSFs. NH1 does not interact with any of the other CSFs due to symmetry. The triplet and singlet interaction matrices are

	$\|T\rangle$	$\|NH2\rangle$	$\|I2\rangle$	$\|I4\rangle$	$\|I6\rangle$	$\|I8\rangle$
$\langle T\|$	$-2K$					
$\langle NH2\|$	$K_{24} - K_{13}$	$2K''$				
$\langle I2\|$	t_{13}	$-t_{13}$	$U - K_{24}$			
$\langle I4\|$	t_{13}	$-t_{13}$	K_{13}	$U - K_{24}$		
$\langle I6\|$	$-t_{24}$	$-t_{24}$	$\alpha - \beta$	$\beta - \gamma$	$U' - K_{13}$	
$\langle I8\|$	$-t_{24}$	$-t_{24}$	$\beta - \gamma$	$\alpha - \beta$	K_{24}	$U' - K_{13}$

	$\|S\rangle$	$\|NH3\rangle$	$\|I1\rangle$	$\|I3\rangle$	$\|I5\rangle$	$\|I7\rangle$
$\langle S\|$	$-2K + K'$					
$\langle NH3\|$	$\sqrt{3}(K'' - K')$	$2K - K'$				
$\langle I1\|$	$-3t_{13}/\sqrt{6}$	$t_{13}/\sqrt{2}$	$U + K_{24}$			
$\langle I3\|$	$-3t_{13}/\sqrt{6}$	$t_{13}/\sqrt{2}$	K_{13}	$U + K_{24}$		
$\langle I5\|$	$3t_{24}/\sqrt{6}$	$-t_{24}/\sqrt{2}$	$\alpha + \beta$	$\beta + \gamma$	$U' + K_{13}$	
$\langle I7\|$	$3t_{24}/\sqrt{6}$	$-t_{24}/\sqrt{2}$	$\beta + \gamma$	$\alpha + \beta$	K_{24}	$U' + K_{13}$

with $\alpha = \langle\varphi_1\varphi_4|1/r_{12}|\varphi_2\varphi_3\rangle - \langle\varphi_1\varphi_4|1/r_{12}|\varphi_3\varphi_2\rangle$; $\beta = \langle\varphi_1\varphi_4|1/r_{12}|\varphi_2\varphi_3\rangle$ and $\gamma = \langle\varphi_1\varphi_2|1/r_{12}|\varphi_4\varphi_3\rangle - \langle\varphi_1\varphi_2|1/r_{12}|\varphi_3\varphi_4\rangle$. E_0 is omitted and the difference between the on-site repulsion integrals U and U' arises from the double occupancy of φ_1 or φ_3 in I_{1-4} *versus* φ_2 or φ_4 in I_{5-8}.

The interaction between the ionic states and the neutral states with Hund coupling cannot break the Landé pattern. This is very easily demonstrated by considering the effect of $I_{1,2}$ on S and T. The diagonalization of the two 2×2 matrices gives

$$E(T) = \frac{1}{2}\left(U \pm \sqrt{U^2 + 4t_{13}^2}\right)$$
$$E(S) = \frac{1}{2}\left(U \pm \sqrt{U^2 + 6t_{13}^2}\right) \tag{5.40}$$

To make it easier to see that these energies perfectly fit the energy differences described with the Heisenberg Hamiltonian, we simplify the expressions with the Taylor expansion used before in Eq. 5.8. The energies of the lowest two states are

$$E(T) = -\frac{t_{13}^2}{U}$$

$$E(S) = -\frac{3}{2}\frac{t_{13}^2}{U} \tag{5.41}$$

It is now trivial to see that $E(T) - E(Q) = 2\big(E(S) - E(T)\big)$. Note that taking into account the interaction of all the CSFs with ionic character leads to more elaborate expressions for the energies of S and T, but the principle is the same.

The simultaneous interaction of the ionic CSFs with S/T and $NH3/NH2$ makes that the non-Hund states gain some weight in the wave function of the lowest triplet and singlet states. This is exactly the same mechanism as in the configuration interaction of singles and doubles. The singles have no direct interaction with the Hartree-Fock determinant due the Brillouin theorem, but they appear in the CI wave function due to an indirect interaction via the doubles.

5.10 Rationalize the relative size for the estimates of J extracted from the singlet-triplet and from the triplet-quintet energy difference. Hint: compare the matrix elements of the ionic determinants with the non-Hund states and take into consideration the relative energy of the non-Hund states involved in the coupling.

To illustrate the above-discussed concepts, we first decompose the magnetic coupling of the Ni-azido complex with angle $\delta = 0$ in Table 5.5. The first column marked with K results from the diagonalization of the model space with only neutral determinants. The effect of the different exchange interactions makes the quintet the lowest state and no (measurable) deviations from the Heisenberg behaviour are observed. The inclusion of the spin polarization introduces important antiferromagnetic contributions but does not break the Landé pattern. By adding the ionic determinants to the CI wave functions of the three lowest spin states, the magnetic coupling further increases as expected. But, more interestingly, we observe a small difference in the estimates of J calculated from the singlet-triplet and the triplet-quintet energy difference. This non-Heisenberg behaviour becomes more pronounced in the CAS+S calculation when the ionic determinants are relaxed, leading to a stronger interaction with the Hund and non-Hund states. When all electron correlation effects are included, the calculated coupling is close to experiment and the deviations are yet a little larger.

It remains to establish which state, singlet or triplet, is most strongly affected by the interaction with the non-Hund states. For this purpose, we have decomposed the DDCI wave functions of the different spin states and listed the coefficients of

Table 5.5 Decomposition of the magnetic coupling of the binuclear Ni-azido complex with $\delta = 0$

	K	K + SP	CAS(4,4)	CAS(4,4)+S	DDCI
$(E_T - E_Q)/2$	2.41	−9.05	−12.62	−55.57	−104.48
$E_T - E_S$	2.41	−9.04	−12.58	−54.92	−101.47

Table 5.6 Decomposition of the DDCI wave function for the singlet, triplet and quintet state of the binuclear Ni-azido complex with three different values of δ

$\delta = 0°$	Quintet	Triplet	Singlet
Hund	0.97227	0.96552	0.94652
Non-Hund	–	0.00110	0.00002
Ionic	–	0.00163	0.00233
$(E_T - E_Q)/2$	−104.48		
$E_S - E_T$	−101.47		
$\delta = 22°$			
Hund	0.97028	0.96565	0.96545
Non-Hund	–	0.00079	$<10^{-5}$
Ionic	–	0.00117	0.00169
$(E_T - E_Q)/2$	−65.92		
$E_S - E_T$	−64.65		
$\delta = 45°$			
Hund	0.96578	0.96482	0.96633
Non-Hund	–	0.00026	$<10^{-5}$
Ionic	–	0.00037	0.00057
$(E_T - E_Q)/2$	−3.69		
$E_S - E_T$	−3.67		

the Hund, non-Hund and ionic CSFs in Table 5.6. If we first focus on the above-discussed case of $\delta = 0$, we see that the largest non-Hund contribution appears in the triplet function. This is in line with the larger matrix element of NH2 with the even-numbered ionic states I_i and the lower relative energy of NH2 (one atomic non-Hund state) with respect to NH3 (atomic non-Hund coupling on both magnetic centers). Hence, it is expected that the non-Hund states stabilize the triplet state more than the singlet, and hence, $E_S - E_T < (E_T - E_Q)/2$ as observed in the Ni-azido complexes.

Table 5.6 also shows that with increasing angle δ the magnetic coupling is strongly reduced, caused by the loss of efficiency of the kinetic exchange mechanism evidenced by the decrease of the coefficient of the ionic determinants in the wave function of the singlet and the triplet wave functions. At the same time, the deviations to the regular Heisenberg spacing are strongly suppressed as are the coefficients of the non-Hund states. This illustrates the role of the indirect coupling of the non-Hund states with the neutral determinants via the ionic ones; without significant contribution of the ionic determinants, i. e. no efficient kinetic exchange, all possible deviations from the Landé pattern of the energies of the lowest spin states are eliminated.

In summary, biquadratic exchange interactions are only expected in complexes with sizeable magnetic interaction, small on-site repulsion U, not too large on-site exchange interaction K and different inter-site interactions for the pairs of electrons on the different magnetic centers: $K_{13} \neq K_{24}$; $t_{13} \neq t_{24}$.

5.4.2 Decomposition of the Four-Center Interactions

The four-spin interaction as discussed in Chap. 3 (Sect. 3.4.2) is the effective matrix element between the determinants $\Phi_I = |a\bar{b}c\bar{d}|$ and $\Phi_J = |\bar{a}b\bar{c}d|$. Since the direct matrix element of the electronic Hamiltonian between them is zero (there are more than two different columns in the determinants), there must be other, indirect interactions that account for the non-zero value of this interaction. In analogy to the *normal* two-center magnetic interaction, we will review the role of the ionic determinants in the effective matrix elements. Figure 5.14 shows one of the pathways that connects Φ_I with Φ_J through three different ionic states. In the first step an electron hops from site A to B to form the ionic determinant Φ_α. The matrix element is

$$\begin{aligned}\langle \Phi_I | \hat{H} | \Phi_\alpha \rangle = \langle a\bar{b}c\bar{d} | \hat{H} | b\bar{b}c\bar{d} \rangle = \langle a | \hat{h} | b \rangle + \text{smaller} \\ \text{two-electron integrals} = t_{ab} = t\end{aligned} \tag{5.42}$$

The two-electron integrals will be detailed in Chap. 6 but are here absorbed into the effective hopping parameter t_{ab}. The relative energy of Φ_α is U, the same parameter as in the analysis of the two-center interaction. The next step transfers an electron with β spin to center C to generate Φ_β with energy U. Assuming a square lattice, the matrix element with Φ_α equals t. The third and fourth step are similar and in total one gets the fourth-order perturbation contribution of this path to the effective matrix element between Φ_I and Φ_J by applying Eq. 5.12.

$$\frac{\langle \Phi_I | \hat{H} | \Phi_\alpha \rangle \langle \Phi_\alpha | \hat{H} | \Phi_\beta \rangle \langle \Phi_\beta | \hat{H} | \Phi_\gamma \rangle \langle \Phi_\gamma | \hat{H} | \Phi_J \rangle}{(E_\alpha - E_J)(E_\beta - E_J)(E_\gamma - E_J)} = \frac{t^4}{U^3} \tag{5.43}$$

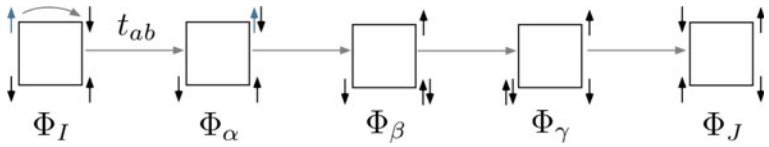

Fig. 5.14 Basic pathway to connect $\Phi_I = |a\bar{b}c\bar{d}|$ with $\Phi_J = |\bar{a}b\bar{c}d|$ via electron hopping among neighboring sites parametrized by $t = t_{ij}$. The relative energies of the intermediate determinants $\Phi_{\alpha,\beta,\gamma}$ is U

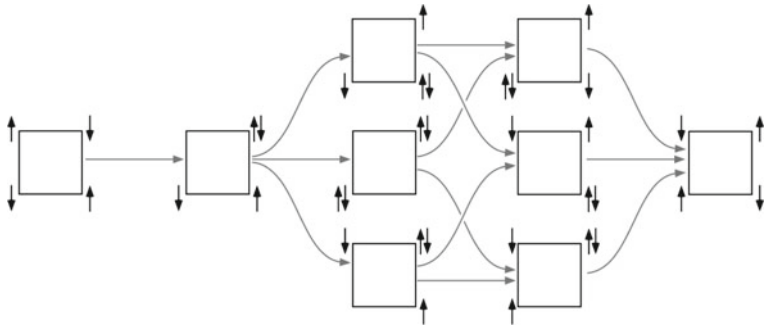

Fig. 5.15 The six pathways that connect $\Phi_I = |a\bar{b}c\bar{d}|$ with $\Phi_J = |\bar{a}bc\bar{d}|$ in a clockwise fashion. The relative energy of all intermediate determinants is U, expect the di-ionic determinant (*third column in the middle*), whose energy can be approximated by $2U$

5.11 Equation 5.43 assumes that the energies of Φ_α and Φ_β are strictly the same. Is this correct? Hint: Assume that A, B, C and D are uncharged in Φ_I and calculate the Coulomb interaction along the path in a simple point charge model.

The path in Fig. 5.14 is not the only possibility to go from Φ_I to Φ_J. In fact, there are 48 different pathways. Twelve of these start with an electron hopping from center A, six with a clockwise circulation and six go in an anti-clockwise fashion. Figure 5.15 shows the six clockwise electron circulations starting at center A, the upper path corresponds to the one that was discussed before. Putting the energy of the di-ionic state—third column in the middle of the figure—at $2U$, the total contribution of the six paths is

$$4 \times \frac{t^4}{U^3} + 2 \times \frac{t^4}{U \cdot 2U \cdot U} = 5\frac{t^4}{U^3} \tag{5.44}$$

The contribution of the anti-clockwise pathways is the same, increasing the prefactor to 10. By accounting for the pathways that start at the other magnetic centers, we can derive the total effective matrix element and a perturbative estimate of J_r

$$\langle \Phi_I | \hat{H}^{eff} | \Phi_J \rangle = 40\frac{t^4}{U^3} \Rightarrow J_r^{pt} = 80\frac{t^4}{U^3} \tag{5.45}$$

5.12 Write down an anti-clockwise path from Φ_I to Φ_J starting at center A that goes through a di-ionic determinant.

The comparison of this expression with the one derived for the ordinary two-center coupling ($4t^2/U$) shows that J_r is expected to be significantly smaller than the interactions described in the standard Heisenberg Hamiltonian, dividing by U^3 instead of U makes the interaction much smaller. However, the very large prefactor in the perturbative estimate makes that the ring exchange is not necessarily negligible in all cases. As long as U is not too large and t sizeable, one can expect significant four-center interactions when the geometry of the system is square-like.

5.4.3 *Complex Interactions with Single Determinant Approaches*

Biquadratic exchange: The isotropic linear magnetic exchange can be calculated in a rather straightforward way with single determinant spin unrestricted methods. Assuming that the BS determinant is a linear combination of the spin states with lowest and highest possible spin moment, the Yamaguchi equation (Eq. 4.85) relates the energies of the BS and HS determinants with J in a straightforward way, independent of the number of unpaired electrons on the magnetic sites involved in the coupling. The biquadratic exchange can however not be addressed from energy differences only, simply because we have only access to one energy difference, obviously too few to determine two parameters.

Instead one can estimate the strength of the biquadratic exchange in an indirect way via the electronic structure parameters U, t and K. To derive the relevant equations we need to compare the expressions of the singlet and triplet states in terms of J and λ given in Eq. 3.75 with their fourth-order perturbation estimates using the matrix elements derived in Sect. 5.4.1. In the first place, we need a common zero of energy. This is easily achieved by putting the energy of the quintet state to zero. The expressions of singlet, triplet and quintet states in terms of J and λ then become

$$\begin{aligned} E(Q) &= 0 \\ E(T) &= 2J \\ E(S) &= 3J + 3\lambda \end{aligned} \tag{5.46}$$

The fourth-order perturbation estimates give us expressions in terms of t, U and K, and hence, we can relate λ to these electronic structure parameters, which can be calculated with spin-unrestricted single determinant methods. To simplify the perturbation estimates we neglect α, β and γ, and all intersite exchange integrals in the interaction matrices derived in Sect. 5.4.1. The interaction matrices for triplet and singlet states then become

	$\|T\rangle$	$\|NH2\rangle$	$\|I2\rangle$	$\|I4\rangle$	$\|I6\rangle$	$\|I8\rangle$
$\langle T\|$	0					
$\langle NH2\|$	0	$2K$				
$\langle I2\|$	t_{13}	$-t_{13}$	U			
$\langle I4\|$	t_{13}	$-t_{13}$	0	U		
$\langle I6\|$	$-t_{24}$	$-t_{24}$	0	0	U'	
$\langle I8\|$	$-t_{24}$	$-t_{24}$	0	0	0	U'

	$\|S\rangle$	$\|NH3\rangle$	$\|I1\rangle$	$\|I3\rangle$	$\|I5\rangle$	$\|I7\rangle$
$\langle S\|$	0					
$\langle NH3\|$	0	$4K$				
$\langle I1\|$	$-3t_{13}/\sqrt{6}$	$t_{13}/\sqrt{2}$	U			
$\langle I3\|$	$-3t_{13}/\sqrt{6}$	$t_{13}/\sqrt{2}$	0	U		
$\langle I5\|$	$3t_{24}/\sqrt{6}$	$-t_{24}/\sqrt{2}$	0	0	U'	
$\langle I7\|$	$3t_{24}/\sqrt{6}$	$-t_{24}/\sqrt{2}$	0	0	0	U'

The second-order correction to the energy is obtained from the expression

$$E^{(2)} = \frac{\langle \Phi_I|\hat{H}|\Phi_\alpha\rangle\langle\Phi_\alpha|\hat{H}|\Phi_I\rangle}{E_I - E_\alpha} \tag{5.47}$$

which becomes

$$E_T^{(2)} = \sum_{i=2,4,6,8} \frac{\langle T|\hat{H}|Ii\rangle\langle Ii|\hat{H}|T\rangle}{-U_i} = -\frac{2t_{13}^2}{U} - \frac{2t_{24}^2}{U'} \tag{5.48}$$

for the triplet and

$$E_S^{(2)} = \sum_{i=1,3,5,7} \frac{\langle S|\hat{H}|Ii\rangle\langle Ii|\hat{H}|S\rangle}{-U_i} = -\frac{3t_{13}^2}{U} - \frac{3t_{24}^2}{U'} \tag{5.49}$$

for the singlet. From these equations we can define $J^{(2)}$, the second-order estimate of J, as $-\frac{t_{13}^2}{U} - \frac{t_{24}^2}{U'}$. The fourth-order contribution is determined with Eq. 5.12 and counts with much more terms, which are summarized below and illustrated for one of the cases in Fig. 5.16.

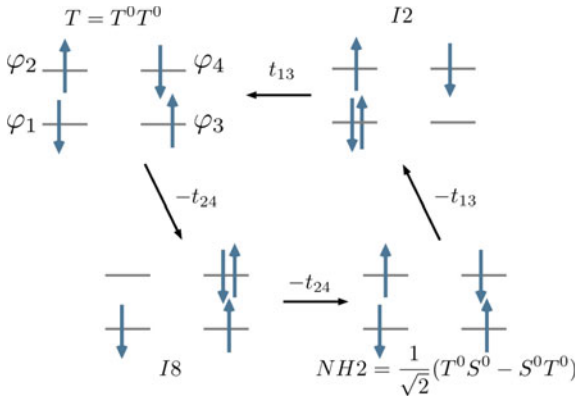

Fig. 5.16 Schematic representation of one of the fourth-order interactions contributing to the energy of the triplet state. The total contribution of this path equals $-t_{13}^2 t_{24}^2/UU'2K$

Φ_I	Φ_α	Φ_β	Φ_γ	Φ_I		Φ_I	Φ_α	Φ_β	Φ_γ	Φ_I	
S	$I1$	$NH3$	$I1$	S	$-\frac{3}{4}t_{13}^4/U^2 4K$	T	$I2$	$NH2$	$I2$	T	$-t_{13}^4/U^2 2K$
			$I3$		$-\frac{3}{4}t_{13}^4/U^2 4K$				$I4$		$-t_{13}^4/U^2 2K$
			$I5$		$-\frac{3}{4}t_{13}^2 t_{24}^2/UU'4K$				$I6$		$t_{13}^2 t_{24}^2/UU'2K$
			$I7$		$-\frac{3}{4}t_{13}^2 t_{24}^2/UU'4K$				$I8$		$t_{13}^2 t_{24}^2/UU'2K$
	$I3$		$I3$		$-\frac{3}{4}t_{13}^4/U^2 4K$		$I4$		$I4$		$-t_{13}^4/U^2 2K$
			$I5$		$-\frac{3}{4}t_{13}^2 t_{24}^2/UU'4K$				$I6$		$t_{13}^2 t_{24}^2/UU'2K$
			$I7$		$-\frac{3}{4}t_{13}^2 t_{24}^2/UU'4K$				$I8$		$t_{13}^2 t_{24}^2/UU'2K$
	$I5$		$I5$		$-\frac{3}{4}t_{24}^4/U'^2 4K$		$I6$		$I6$		$-t_{24}^4/U'^2 2K$
			$I7$		$-\frac{3}{4}t_{24}^4/U'^2 4K$				$I8$		$t_{24}^2/U'^2 2K$
	$I7$		$I7$		$-\frac{3}{4}t_{24}^4/U'^2 4K$		$I6$		$I6$		$-t_{24}^4/U'^2 2K$

The terms with the ionic states interchanged ($\Phi_\alpha = I3$, $\Phi_\gamma = I1$, etc.) should also be added to the perturbational estimate. This is easily done by multiplying all the terms by two, except the ones with $\Phi_\alpha = \Phi_\gamma$. Now the following corrections arise

$$E_T^{(4)} = \frac{2t_{13}^4}{U^2 K} + \frac{2t_{24}^4}{U'^2 K} - \frac{4t_{13}^2 t_{24}^2}{UU'K} = \frac{2B}{K} \tag{5.50}$$

$$E_S^{(4)} = -\frac{3}{4}\frac{t_{13}^4}{U^2 K} - \frac{3}{4}\frac{t_{24}^4}{U'^2 K} - \frac{3}{2}\frac{t_{13}^2 t_{24}^2}{UU'K} = -\frac{3J^{(2)2}}{4K} \tag{5.51}$$

with $B = t_{13}^2/U - t_{24}^2/U'$. Then the total perturbative estimate for the singlet and triplet energies are

$$E_T = E_T^{(2)} + E_T^{(4)} = -\frac{2t_{13}^2}{U} - \frac{2t_{24}^2}{U'} - \frac{2B^2}{K} = 2J^{(2)} - \frac{2B^2}{K} \tag{5.52}$$

$$E_S = E_S^{(2)} + E_S^{(4)} = -\frac{3t_{13}^2}{U} - \frac{3t_{24}^2}{U'} - \frac{3J^2}{4K} = 3J^{(2)} - \frac{3J^{(2)2}}{4K} \tag{5.53}$$

The comparison with the expression for the singlet and triplet energy eigenvalues of the Heisenberg Hamiltonian with biquadratic terms leads to a fourth-order estimate of J as

$$J = J^{(2)} - \frac{B^2}{K} \tag{5.54}$$

Then from the singlet energy we get

$$E_S = 3J + 3\lambda = 3\left(J^{(2)} - \frac{B^2}{K}\right) + 3\lambda = 3J^{(2)} - \frac{3J^{(2)2}}{4K} \tag{5.55}$$

from which the perturbative expression for λ in terms of t, U and K can be extracted

$$\lambda = \frac{B^2}{3K} - \frac{J^{(2)2}}{4K} \tag{5.56}$$

The next step concerns the calculation of the energy of a collection of spin unrestricted determinants with different occupations and relate their energies to the electronic structure parameters in order to calculate the λ parameter and in this way obtain a measure for the biquadratic interaction strength from methods like DFT (Fig. 5.17).

Assuming that $U = U'$, the energies of the following five determinants define the parameters that appear in the perturbative expressions of B and J, which in turn lead to an estimate of λ, the biquadratic exchange parameter.

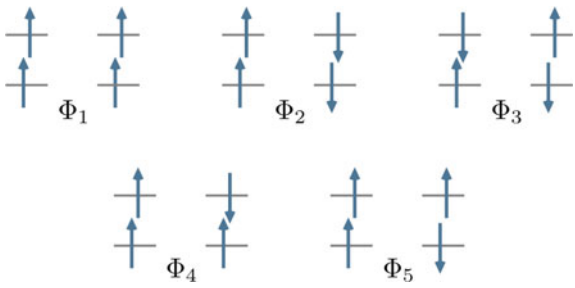

Fig. 5.17 The five determinants that are needed to calculate the electronic structure parameters that define B and J in the perturbative expression of the biquadratic exchange strength

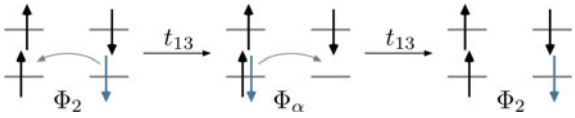

Fig. 5.18 One of the second-order contributions to the energy of Φ_2. This path contributes $t_{13}^2/-U$

$$M_S = 2: \quad \Phi_1 = |\varphi_1\varphi_2\varphi_3\varphi_4| \qquad E_1^{(2)} = 0 \tag{5.57}$$

$$M_S = 0: \quad \Phi_2 = |\varphi_1\varphi_2\overline{\varphi}_3\overline{\varphi}_4| \qquad E_2^{(2)} = -\frac{2(t_{13}^2 + t_{24}^2)}{U} \tag{5.58}$$

$$\Phi_3 = |\varphi_1\overline{\varphi}_2\overline{\varphi}_3\varphi_4| \qquad E_3^{(2)} = 2K - \frac{2(t_{13}^2 + t_{24}^2)}{U} \tag{5.59}$$

$$M_S = 1: \quad \Phi_4 = |\varphi_1\varphi_2\varphi_3\overline{\varphi}_4| \qquad E_4^{(2)} = K - \frac{2t_{24}^2}{U} \tag{5.60}$$

$$\Phi_5 = |\varphi_1\varphi_2\overline{\varphi}_3\varphi_4| \qquad E_5^{(2)} = K - \frac{2t_{13}^2}{U} \tag{5.61}$$

The listed energies are the sum of the zeroth-order energies and second-order corrections. The latter are calculated by taking into account all possible interactions of these determinants with the ionic determinants, which are assumed to be degenerate with energy U relative to Φ_1. One example is given in Fig. 5.18, the rest is completely analogous. The zeroth-order energies $\langle \Phi_I | \hat{H} | \Phi_I \rangle$ only count the number of on-site exchange interactions K, all other terms are neglected or the same as in the reference energy $E_1^{(0)}$.

5.13 Write down the two ionic determinants that interact with Φ_4 and calculate the interaction matrix elements.

Four-center interactions: In Chap. 3, we have seen how the four-center interactions can be extracted using an effective Hamiltonian spanned by the six $M_S = 0$ determinants. To address the ring exchange within a spin unrestricted setting, this model space is no longer sufficient, but has to be extended with the $M_S = 2$ and the four $M_S = 1$ determinants. In any standard implementation of density functional theory, the main area of spin unrestricted methods, one has only access to the diagonal elements of this 11×11 model Hamiltonian; matrix elements between different determinants are not routinely calculated in most quantum chemistry packages. In addition, it should be realized that the four $M_S = 1$ determinants are all degenerate and as was shown in Eq. 3.84, the six $M_S = 0$ determinants are degenerate in pairs. Hence, one can count with at most five energies, i.e. four energy differences that can be used to determine four independent parameters. It is therefore intrinsically impossible to determine the interaction strength of the three cyclic permutations defined in Fig. 3.14, as can in principle be done with wave function based methods through the construction of a numerical effective Hamiltonian. However, in any practical case

there is only one sizeable four-center interaction, namely the one with the $\hat{P}_{1234}$ operator associated to it.

The expectation values of the $M_S = 0$ determinants can be found in Eq. 3.84, but for the $M_S = 1$ and $M_S = 2$ determinants we will derive them here. Among the four degenerate $M_S = 1$ determinants we will focus on $|abc\overline{d}|$, or $|\alpha\alpha\alpha\beta|$ in a spin-only notation. With the following ingredients for the two-center interactions:

$$\begin{aligned}
-J_1(\hat{S}_A\hat{S}_B + \hat{S}_C\hat{S}_D)\alpha\alpha\alpha\beta &= -J_1\left(\frac{1}{4}\alpha\alpha\alpha\beta + \frac{1}{2}\alpha\alpha\beta\alpha - \frac{1}{4}\alpha\alpha\alpha\beta\right) \\
-J_2(\hat{S}_A\hat{S}_D + \hat{S}_B\hat{S}_C)\alpha\alpha\alpha\beta &= -J_2\left(\frac{1}{2}\beta\alpha\alpha\alpha - \frac{1}{4}\alpha\alpha\alpha\beta + \frac{1}{4}\alpha\alpha\alpha\beta\right) \\
-J_3(\hat{S}_A\hat{S}_D + \hat{S}_B\hat{S}_C)\alpha\alpha\alpha\beta &= -J_3\left(\frac{1}{4}\alpha\alpha\alpha\beta + \frac{1}{2}\alpha\beta\alpha\beta - \frac{1}{4}\alpha\alpha\alpha\beta\right)
\end{aligned} \tag{5.62}$$

and for the four-center interaction:

$$\begin{aligned}
J_r(\hat{S}_A\hat{S}_B)(\hat{S}_C\hat{S}_D)\alpha\alpha\alpha\beta &= J_r(\hat{S}_A\hat{S}_B)\left(\frac{1}{2}\alpha\alpha\beta\alpha - \frac{1}{4}\alpha\alpha\alpha\beta\right) \\
&= J_r\left(\frac{1}{8}\alpha\alpha\beta\alpha - \frac{1}{16}\alpha\alpha\alpha\beta\right) \\
J_r(\hat{S}_A\hat{S}_D)(\hat{S}_B\hat{S}_C)\alpha\alpha\alpha\beta &= J_r(\hat{S}_A\hat{S}_D)\left(\frac{1}{4}\alpha\alpha\alpha\beta\right) \\
&= J_r\left(\frac{1}{8}\beta\alpha\alpha\alpha - \frac{1}{16}\alpha\alpha\alpha\beta\right) \\
-J_r(\hat{S}_A\hat{S}_C)(\hat{S}_B\hat{S}_D)\alpha\alpha\alpha\beta &= -J_r(\hat{S}_A\hat{S}_C)\left(\frac{1}{2}\alpha\beta\alpha\alpha - \frac{1}{4}\alpha\alpha\alpha\beta\right) \\
&= -J_r\left(\frac{1}{8}\alpha\beta\alpha\alpha - \frac{1}{16}\alpha\alpha\alpha\beta\right)
\end{aligned} \tag{5.63}$$

the matrix element becomes

$$\langle\alpha\alpha\alpha\beta|\hat{H}|\alpha\alpha\alpha\beta\rangle = -\frac{1}{16}J_r \tag{5.64}$$

Applying the same procedure to $|\alpha\alpha\alpha\alpha|$ leads to

$$\langle\alpha\alpha\alpha\alpha|\hat{H}|\alpha\alpha\alpha\alpha\rangle = -\frac{1}{2}(J_1 + J_2 + J_3) + \frac{1}{16}J_r \tag{5.65}$$

5.14 Check the matrix element of the $M_S = 2$ determinant of the spin Hamiltonian given in Eq. 3.83.

Taking the expectation value of the $M_S = 2$ determinant as zero of energy, the following relations emerge to determine the four parameters

$$\begin{aligned} E(|a\overline{b}c\overline{d}|) - E(|abcd|) &= J_1 + J_2 \\ E(|ab\overline{c}\overline{d}|) - E(|abcd|) &= J_1 + J_3 \\ E(|a\overline{b}\overline{c}d|) - E(|abcd|) &= J_2 + J_3 \\ E(|abc\overline{d}|) - E(|abcd|) &= \frac{1}{2}(J_1 + J_2 + J_3) - \frac{1}{8}J_r \end{aligned} \tag{5.66}$$

Hence, the extraction of the four-spin cyclic exchange parameter within the spin-unrestricted setting of the DFT approach relies on obtaining converged solutions for the determinants with the required spin distributions, which is not always a trivial task.

Problems

5.1 Zeroth-order description. Write down the matrix of the model space that only considers neutral determinants expressed in local orbitals. Diagonalize the matrix and calculate the singlet-triplet energy difference. What is the state of lowest energy?

5.2 Construction of the CAS(2,2)CI matrix in the symmetry adapted CSF basis. The CASCI matrix given in Eq. 5.4 uses the four $M_S = 0$ determinants as basis. The matrix can be greatly simplified by a basis set change using symmetry adapted CSFs.

a. Write down the four symmetry adapted CSFs that arise from the linear combinations of the four $M_S = 0$ determinants. The expressions of the states after configuration interaction given in Eq. 5.5 may give a hint on the CSFs.
b. Calculate the energy expectation values of the four CSFs and place them on the diagonal of the matrix.
c. Identify the CSFs as singlet or triplet spin eigenfunctions and label them by *gerade/ungerade* spatial symmetry, assuming that the system has an inversion center. How many off-diagonal elements have non-zero value?
d. Calculate the remaining matrix elements to complete the CAS(2,2)CI matrix.

5.3 Spin contamination of the BS state. The relaxation of the magnetic orbitals of the BS determinant in the field of the frozen ROKS core orbitals introduces spin contamination. The amount of spin contamination can be determined analytically by rewriting Eq. 5.26 in terms of spin adapted CSFs instead of the neutral and ionic valence bond structures.

1. Which term in Eq. 5.26 is an eigenfunction of $\hat{S}^2$. Give the eigenvalue of this term.
2. The two other terms have to be written in the form of the singlet $\left(|a\overline{b}| + |b\overline{a}|\right)$ and triplet $\left(|a\overline{b}| - |b\overline{a}|\right)$ CSFs. Use the trigonometric relations $\sin^2\phi + \cos^2\phi = 1$ and

$\sin^2\phi - \cos^2\phi = \cos(2\phi)$. Hint: Add and subtract $\frac{1}{2}\cos^2\alpha|b\overline{a}| + \frac{1}{2}\sin^2\alpha|a\overline{b}|$ and split the first two terms of Eq. 5.26 in halfs. Then, order the terms to form the given trigonometric relations.

3. Calculate $\langle\Phi_{BS}|\hat{S}^2|\Phi_{BS}\rangle$ using the above derived expression $\Phi_{BS} = (|a\overline{b}| + |b\overline{a}|)/2 + (|a\overline{b}| - |b\overline{a}|)\cos(2\alpha)/2 + (|a\overline{a}| + |b\overline{b}|)\sin\alpha\cos\alpha$.

5.4 Kinetic exchange by second-order perturbation theory. Make a second-order estimate of the singlet energy taking into account the interaction between $S = \frac{1}{\sqrt{2}}\left(|a\overline{b}| + |b\overline{a}|\right)$ and the ionic states $I_1 = \frac{1}{\sqrt{2}}\left(|a\overline{a}| + |b\overline{b}|\right)$ and $I_2 = \frac{1}{\sqrt{2}}\left(|a\overline{a}| - |b\overline{b}|\right)$. The energy of the triplet, $T = \frac{1}{\sqrt{2}}\left(|a\overline{b}| - |b\overline{a}|\right)$, equals $E_{ref} - K_{ab}$ and should be taken as reference.

5.5 Biquadratic exchange versus t_{13}/t_{24}. Express the perturbative estimate of λ (Eq. 5.56) in terms of t_{13} and t_{24} with a common denominator for the two terms. Determine for which values of t_{13} and t_{24} the biquadratic exchange vanishes and for which values it can be expected to be maximal.

5.6 Estimating $\mathbf{J_r}$. Accurate calculations on a polynuclear paramagnetic compound with four $S = \frac{1}{2}$ magnetic centers indicate that the only significant interactions are the following bilinear isotropic interactions: $J_{12} = J_{34} = -25.1$ meV, and $J_{23} = J_{14} = -39.5$ meV. Nevertheless, the experimental temperature dependence of the magnetic susceptibility could not be fitted satisfactorily with these values. Provide a perturbational estimate for the four-center cyclic exchange to improve the fitting (extra data: $U = 5.3$ eV).

References

1. J. Cabrero, C. de Graaf, E. Bordas, R. Caballol, J.P. Malrieu, Chem. Eur. J. **9**, 2307 (2003)
2. C.J. Calzado, J. Cabrero, J.P. Malrieu, R. Caballol, J. Chem. Phys. **116**(7), 2728 (2002)
3. C.J. Calzado, J. Cabrero, J.P. Malrieu, R. Caballol, J. Chem. Phys. **116**(10), 3985 (2002)
4. C.J. Calzado, C. Angeli, D. Taratiel, R. Caballol, J.P. Malrieu, J. Chem. Phys. **131**, 044327 (2009)
5. E. Coulaud, J.P. Malrieu, N. Guihéry, N. Ferré, J. Chem. Theory Comput. **9**, 3429 (2013)
6. R. Bastardis, N. Guihéry, C. de Graaf, J. Chem. Phys. **129**, 104102 (2008)